

Superconductivity with High Upper Critical Field in the Cubic Centrosymmetric η -Carbide $\text{Nb}_4\text{Rh}_2\text{C}_{1-\delta}$

KeYuan Ma,[†] Karolina Gornicka,[‡] Robin Lefèvre,[†] Yikai Yang,[¶] Henrik Rønnow,[¶]
Harald O. Jeschke,[§] Tomasz Klimczuk,[‡] Fabian O. von Rohr^{†*}

[†] Department of Chemistry, University of Zurich, CH-8057 Zurich, Switzerland

[‡] Faculty of Applied Physics and Mathematics, Gdansk University of Technology,
Gdansk 80-233, Poland

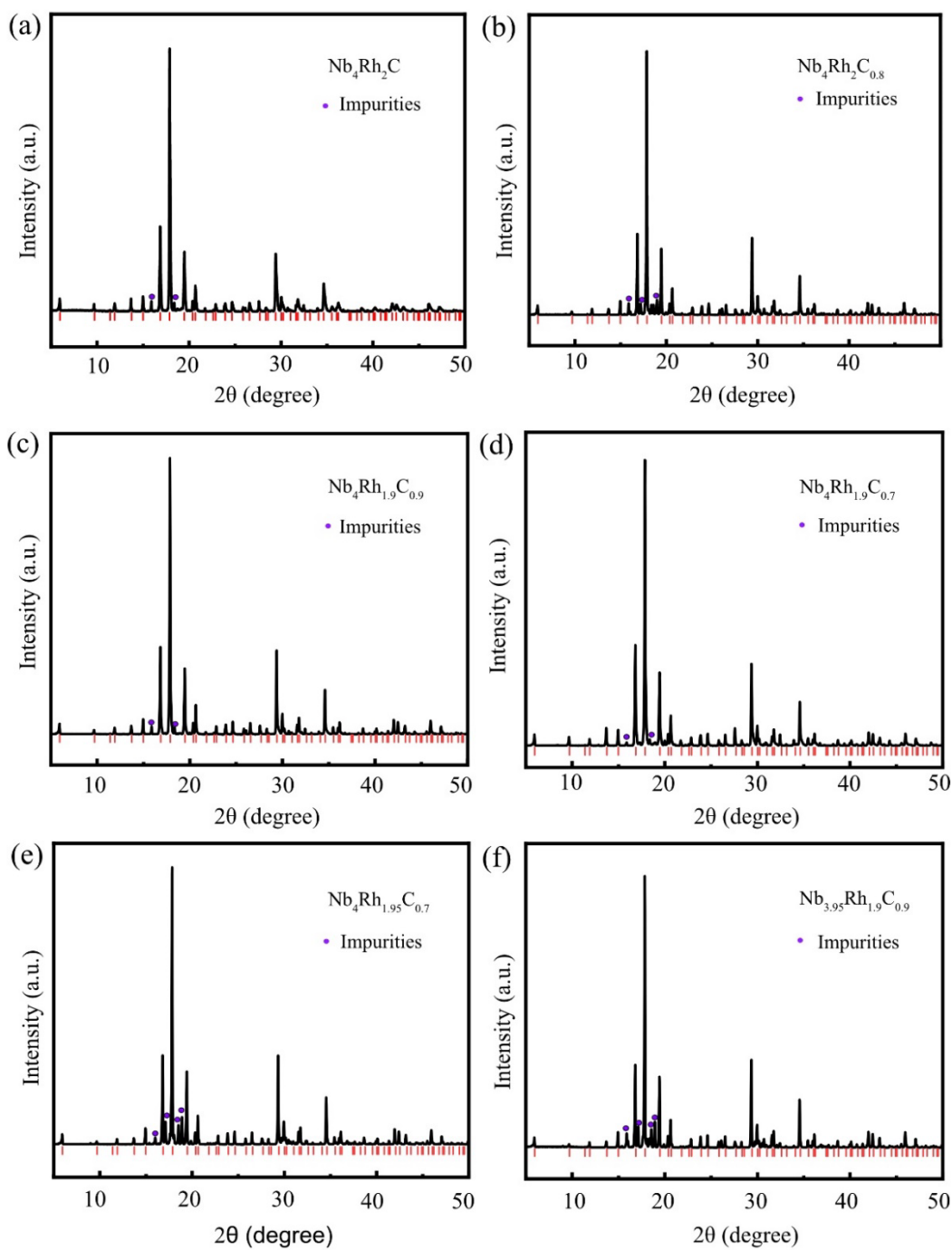
[¶] Institute of Physics, Ecole Polytechnique Fédérale de Lausanne (EPFL), CH-1015
Lausanne, Switzerland

[§] Research Institute for Interdisciplinary Science, Okayama University, Okayama 700-
8530, Japan

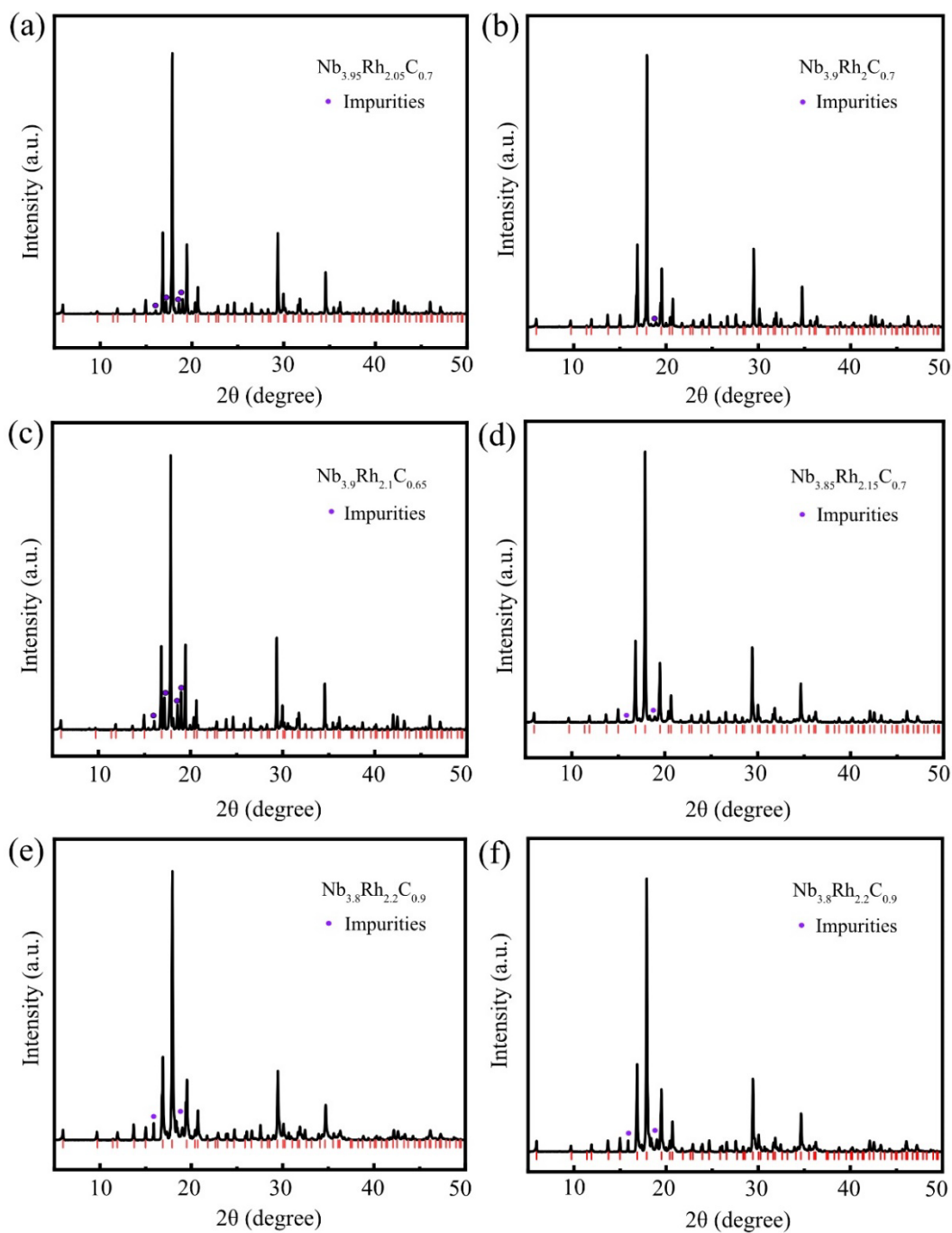
* To whom correspondence should be addressed. E-mail: fabian.vonrohr@chem.uzh.ch

Synthesis of phase pure sample

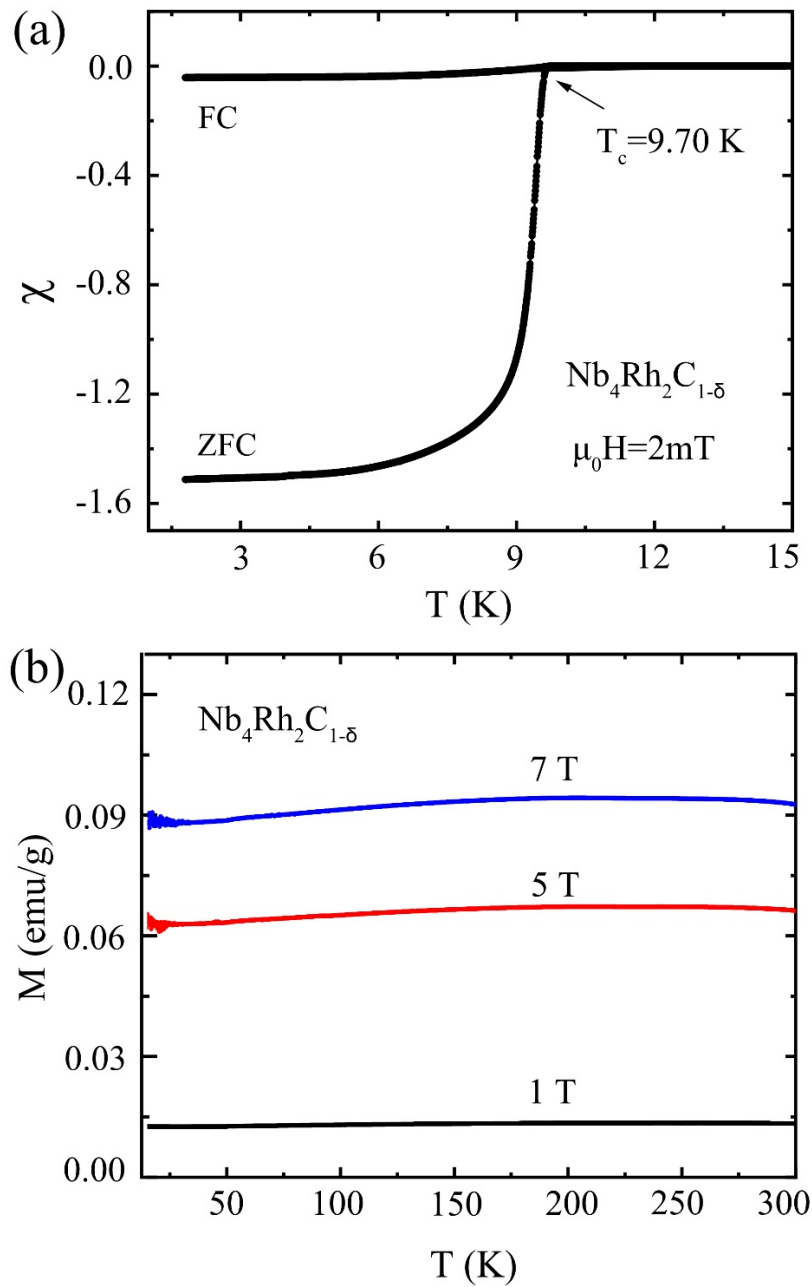
In order to obtain phase pure samples, we synthesized a series of samples with varying compositions (see Sfig. 1-2). It was found that the development of optimized synthesis conditions was crucial for the realization of phase pure samples. Pure sample is obtained when the carbon is set to be 0.7, more or less carbon will lead to the formation of other impurities, indicating carbon has a solubility in filling up the interstitial positions to stabilize the η -carbide crystal structure. Efforts attempting to replace carbon with nitrogen or oxygen were failed. From the composition varying synthesis, we find carbon is the only interstitial atoms that can stabilize $\text{Nb}_4\text{Rh}_2\text{C}_{1-\delta}$ in the η -carbide crystal structure, and proper carbon deficiency is necessary to obtain phase pure samples.



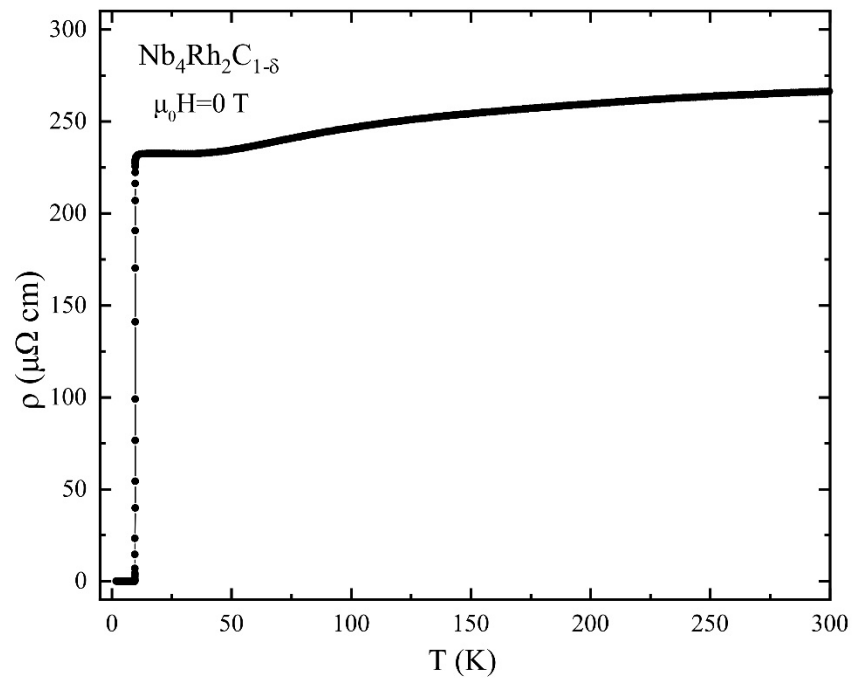
S-Figure 1. PXRD patterns of the products with varying starting chemical compositions



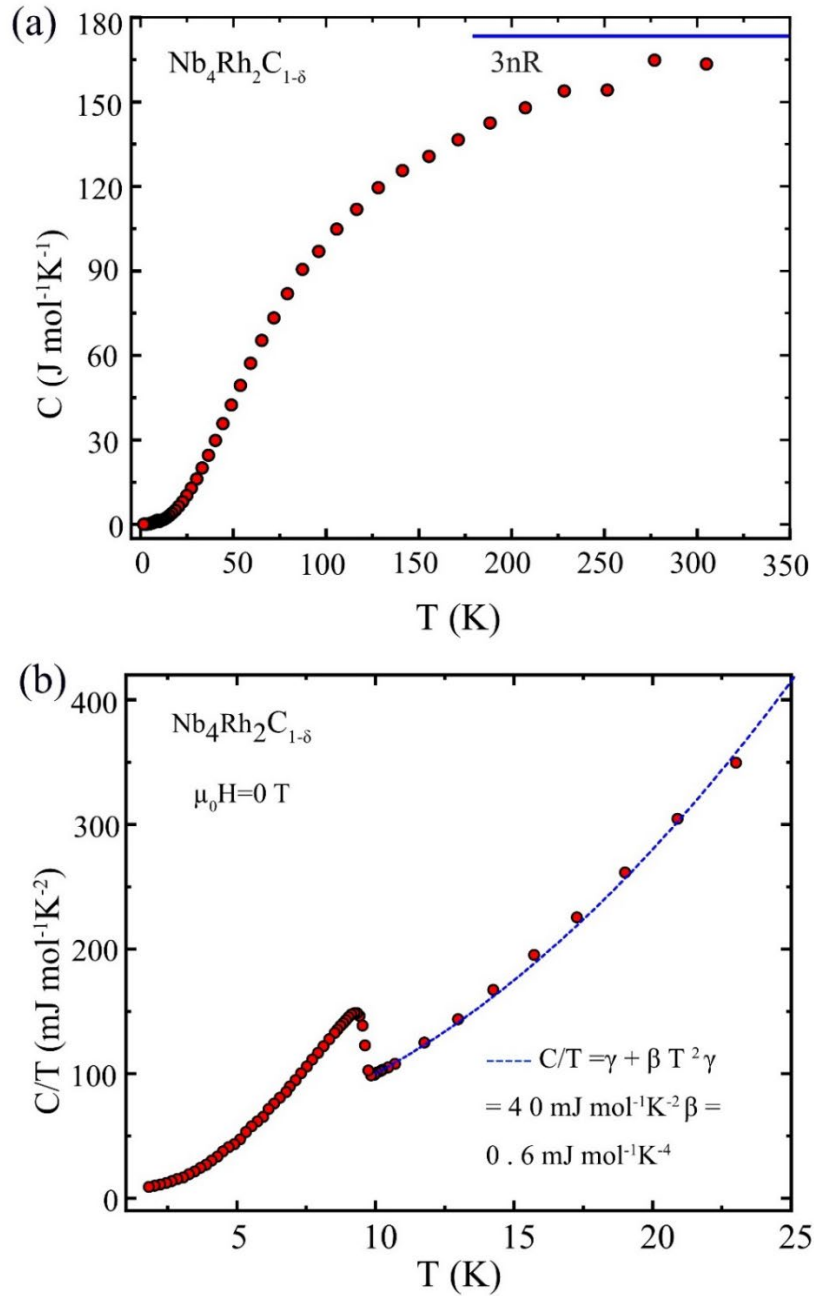
S-Figure 2. PXRD patterns of the products with varying starting chemical compositions



S-Figure 3. (a) Temperature dependence of the magnetic susceptibility in zero field cooled (ZFC) and field cooled (FC) modes for $\text{Nb}_4\text{Rh}_2\text{C}_{1-\delta}$ and (b) normal state magnetization of $\text{Nb}_4\text{Rh}_2\text{C}_{1-\delta}$ in a field of $\mu_0 H = 1$ T, 5 T and 7 T between 10 to 300 K.



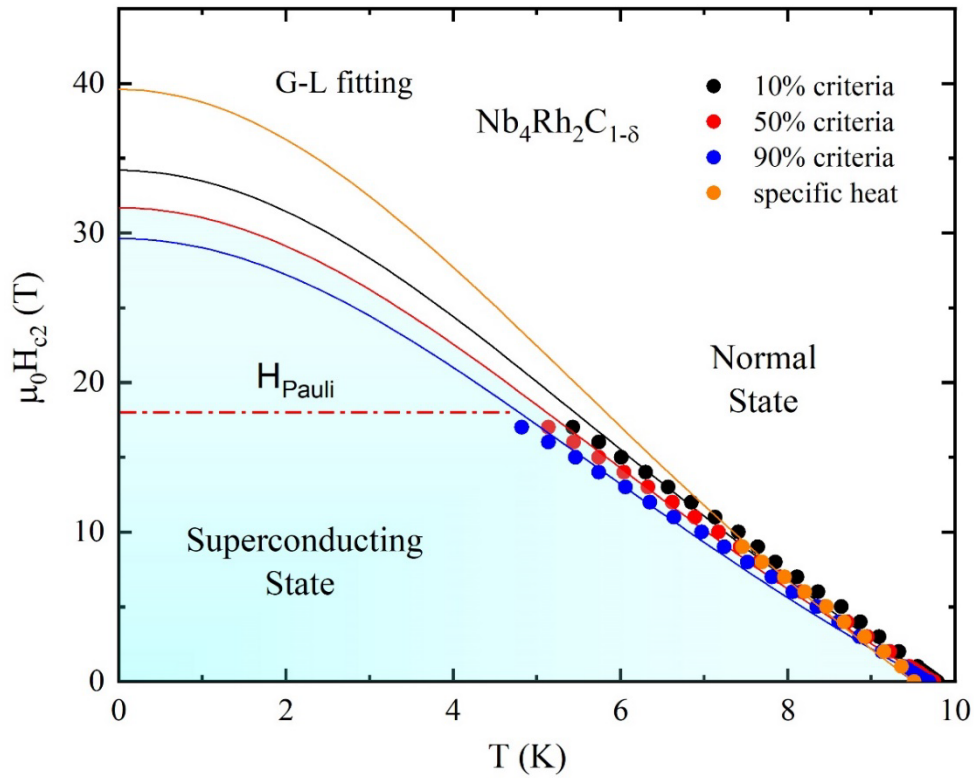
S-Figure 4. Resistivity of $\text{Nb}_4\text{Rh}_2\text{C}_{1-\delta}$ in a field of $\mu_0 H = 0$ T between 2 to 300 K



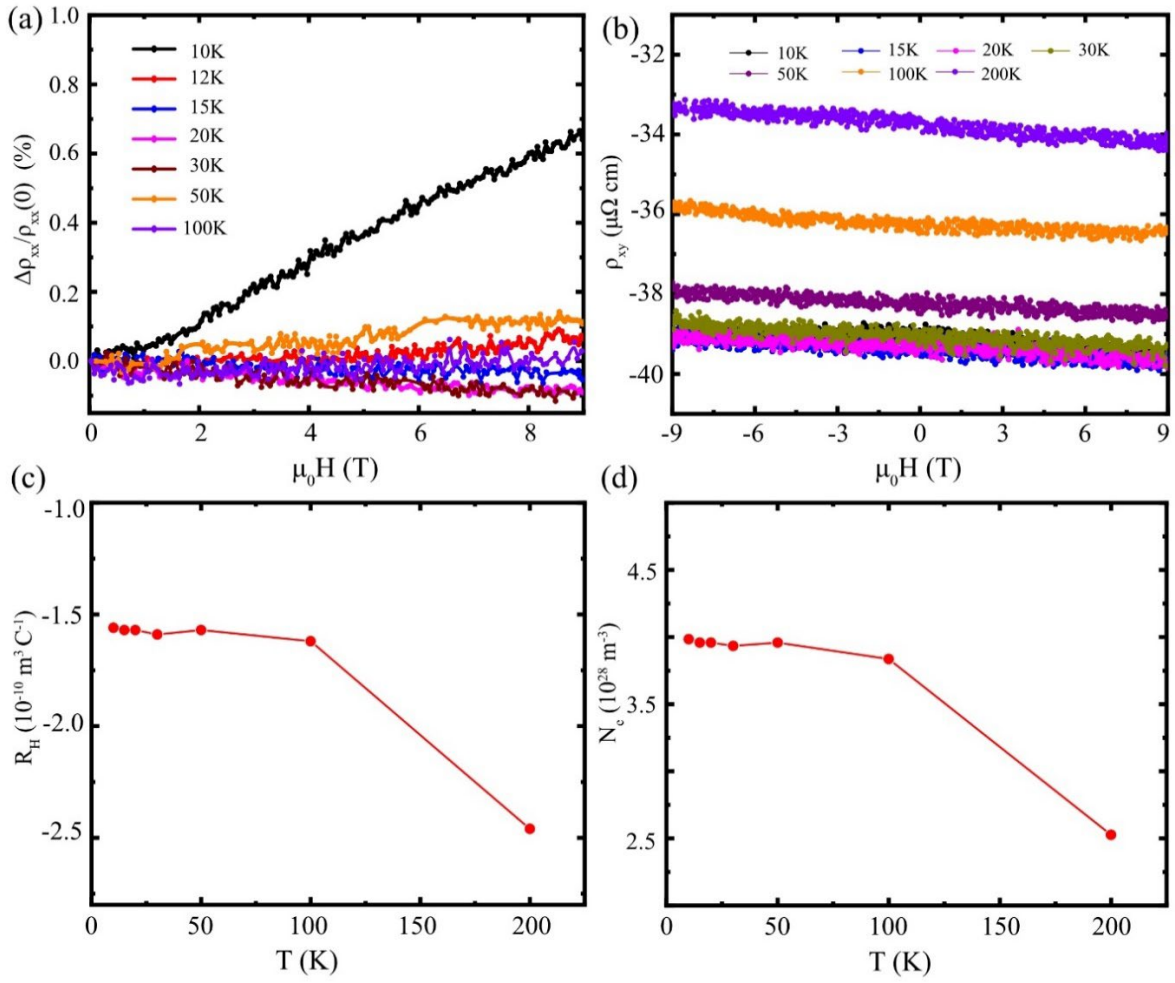
S-Figure 5. Temperature-dependent specific heat capacities $C(T)$ of $\text{Nb}_4\text{Rh}_2\text{C}_{1-\delta}$ between 2 K to 320 K. The data between 10 K to 25 K is plotted in a C/T vs. T representation. The dotted line corresponds to a fit of the normal state specific heat capacities, according to equation $C/T = (C_{el} + C_{ph})/T = \gamma + \beta T^2$.

Here, the upper critical field $H_{c2}(0)$ was determined using the Ginzburg-Landau (GL) model, with $t=T/T_c$ being the reduced temperature:

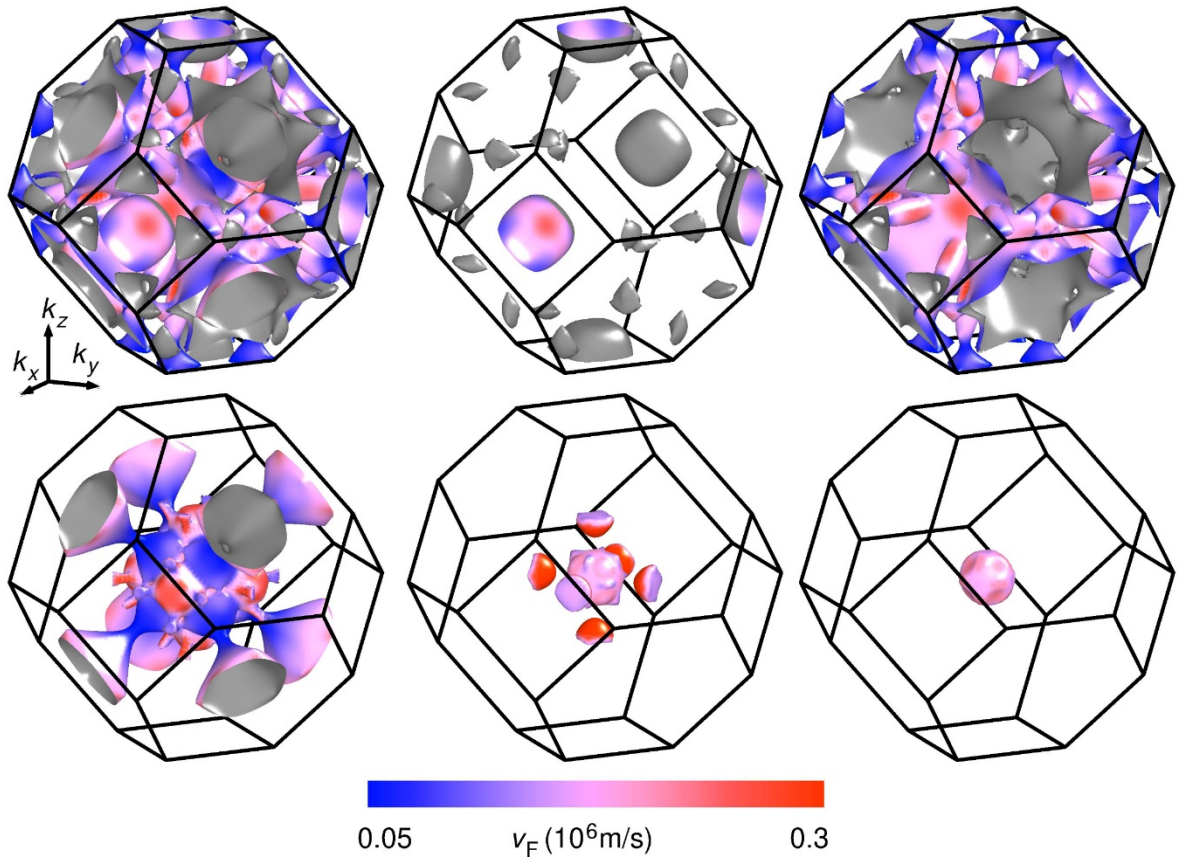
$$H_{c2}(T) = H_{c2}(0) \frac{1 - t^2}{1 + t^2}$$



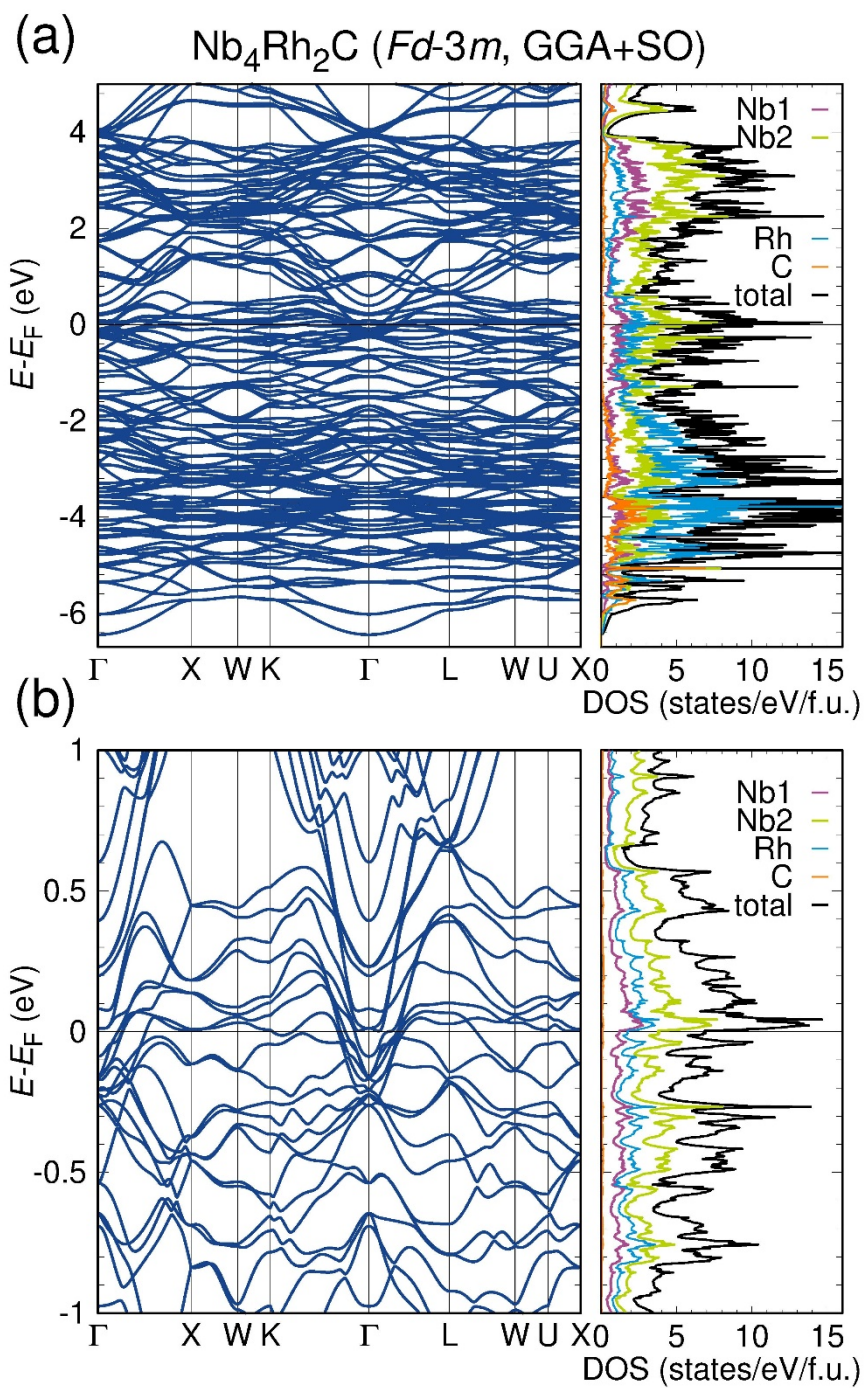
S-Figure 6. Upper critical fields of $\text{Nb}_4\text{Rh}_2\text{C}_{1-\delta}$ determined by the 10%, 50%, 90% criterion with magnetic field up to 17 T and specific heat with Ginzburg-Landau formalism.



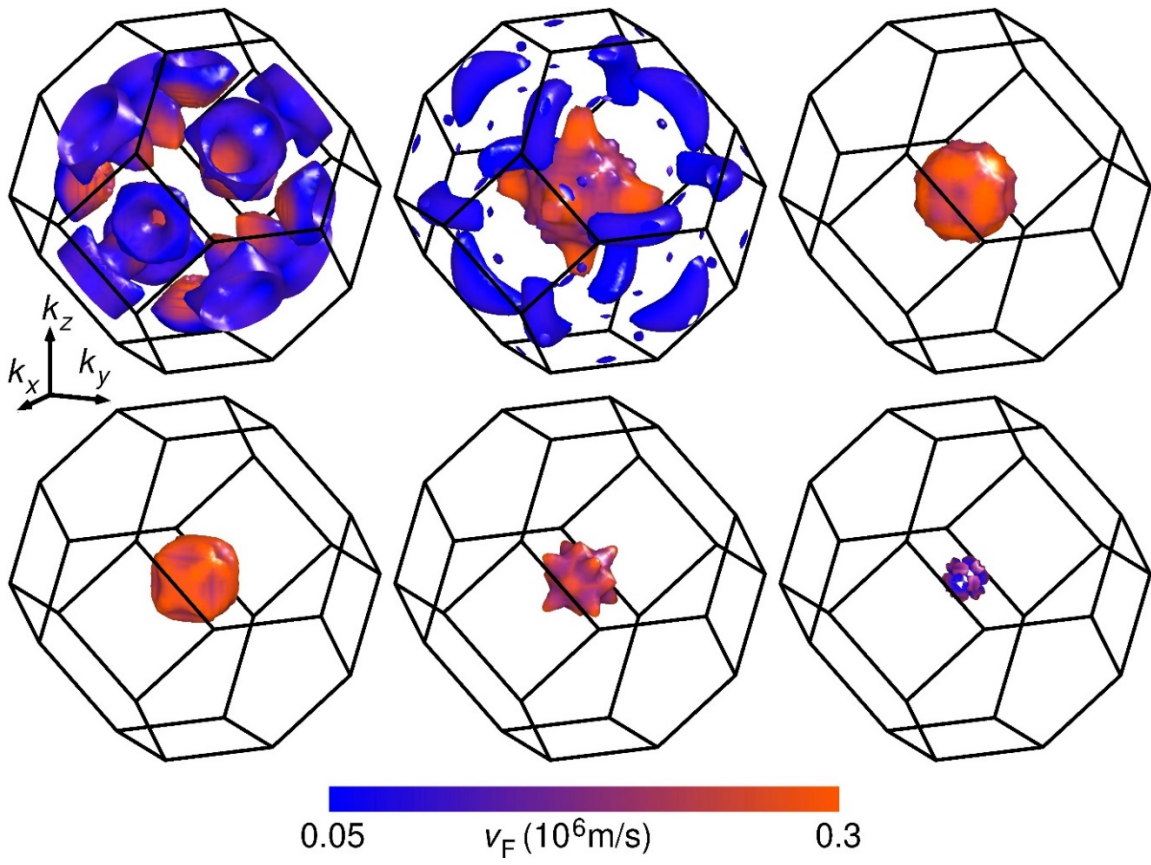
S-Figure 7. (a) Temperature-dependent magnetoresistance, (b) Magnetic field dependence of the transverse resistivity ρ_{xy} at different temperatures, (c) Temperature dependence of Hall coefficient R_H , and (d) Temperature dependence of Carrier densities in $\text{Nb}_4\text{Rh}_2\text{C}_{1-\delta}$.



S-Figure 8. Calculated Fermi surface for $\text{Nb}_4\text{Rh}_2\text{C}_{1-\delta}$ with $\delta=0.3$



S-Figure 9. GGA+SO calculation.



S-Figure 10. Calculated Fermi surface for $\text{Nb}_4\text{Rh}_2\text{C}_{1-\delta}$ with $\delta=0$